## Title

Whole-vessel coronary 18F-sodium fluoride PET for assessment of the global coronary microcalcification burden



## Journal

European Journal of Nuclear Medicine and Molecular Imaging, 47(7)

## ISSN

1619-7070

## Authors

Kwiecinski, Jacek
Cadet, Sebastien
Daghem, Marwa
et al.

## Publication Date

2020-07-01

## DOI

10.1007/s00259-019-04667-z

Peer reviewed

HHS Public Access

Author manuscript

*Eur J Nucl Med Mol Imaging*. Author manuscript; available in PMC 2021 July 01.

Published in final edited form as:

*Eur J Nucl Med Mol Imaging*. 2020 July ; 47(7): 1736–1745. doi:10.1007/s00259-019-04667-z.

# Whole-vessel coronary $^{18}$F-sodium fluoride PET for assessment of the global coronary microcalcification burden

**Jacek Kwiecinski**[a,b] **[First Author] [Resident]**, **Sebastien Cadet**[a], **Marwa Daghem**[c], **Martin L Lassen**[a], **Damini Dey**[a], **Marc R Dweck**[c], **Daniel S Berman**[a], **David E Newby**[c], **Piotr J Slomka**[a]

[a]Department of Imaging (Division of Nuclear Medicine), Medicine, and Biomedical Sciences, Cedars-Sinai Medical Center, Los Angeles, CA, USA; [b]Department of Interventional Cardiology and Angiology, Institute of Cardiology, Warsaw, Poland [c]BHF Centre for Cardiovascular Science, University of Edinburgh, Edinburgh, United Kingdom

## Abstract

**Purpose—**$^{18}$F-sodium fluoride ($^{18}$F-NaF) has shown promise in assessing disease activity in coronary arteries, but currently used measured of activity – such as maximum target to background ratio (TBRmax) -are defined by single pixel count values. We aimed to develop a novel coronary-specific measure of $^{18}$F-NaF PET reflecting activity throughout the entire coronary vasculature (coronary microcalcification activity [CMA]),

**Methods—**Patients with recent myocardial infarction and multi-vessel coronary artery disease underwent $^{18}$F-NaF PET and coronary CTA. We assessed the association between coronary $^{18}$F-NaF uptake (both TBRmax and CMA) and coronary artery calcium scores (CACS) as well as low attenuation plaque (LAP, attenuation <30 Hounsfield units) volume.

**Results—**In 50 patients (64% males, 63±7 years) CMA and TBRmax were higher in vessels with LAP compared to those without LAP (1.09 [0.02, 2.34] versus 0.0 [0.0, 0.0], p<0.001 and 1.23 [1.16, 1.37] versus 1.04 [0.93, 1.11], p<0.001). Compared to a TBRmax threshold of 1.25, CMA > 0 had a higher diagnostic accuracy for detection of LAP: sensitivity of 93.1 (83.3–98.1)% versus 58.6 (44.9–71.4)% and a specificity of 95.7 (88.0–99.1)% versus 80.0 (68.7–88.6)% (both p<0.001).



**Address for Correspondence:** Piotr J. Slomka, PhD, Artificial Intelligence in Medicine Program, Cedars-Sinai Medical Center, 8700 Beverly Blvd, Ste A047N, Los Angeles, CA 90048, USA, piotr.slomka@cshs.org, Phone: 310-423-4348 Fax: 310-423-0173.
**First Author:** Jacek Kwiecinski, MD, PhD, Department of Interventional Cardiology and Angiology, Institute of Cardiology, Alpejska 42, 04-628 Warsaw, Poland, jkwiecinski@ikard.pl, Phone: +48 22 343 41 27 Fax: +48 22 613 38 19, Resident



Disclosures:
DEN (CH/09/002, RE/13/3/30183) and MRD (FS/14/78/31020) are supported by the British Heart Foundation. DEN is the recipient of a Wellcome Trust Senior Investigator Award (WT103782AIA) and MRD of Sir Jules Thorn Award for Biomedical Research Award (2015). DSB, DD, GG and PJS receive software royalties from Cedars–Sinai Medical Center. All other authors have nothing to disclose.

$^{18}$F-NaF uptake assessed by CMA correlated more closely with LAP (r=0.86,p<0.001) than the CT calcium score (r=0.39,p<0.001), with these associations outperforming those observed for TBRmax values (LAP r=0.63,p<0.001; CT calcium score r=0.30,p<0.001).

**Conclusions—**Automated assessment of disease activity across the entire coronary vasculature is feasible using $^{18}$F-NaF CMA, providing a single measurement that has closer agreement with CT markers of plaque vulnerability than more traditional measures of plaque activity.

### Keywords

$^{18}$F-NaF; vulnerable plaque; PET; coronary artery disease

## Introduction

Cardiovascular atherosclerotic disease is the leading cause of death globally [1]. In the past decade, enormous efforts have been undertaken to enable the detection of high-risk coronary artery plaques. While identification of high-risk lesions has traditionally relied on structural intravascular coronary artery imaging or computed tomography (CT) angiography, recently the assessment of plaque biological activity and vulnerability has gained major interest [2–8]. In particular, positron emission tomography (PET) has provided insight into coronary inflammation and micro-calcification activity [9–11]. To date, PET image analysis was typically performed using a maximum activity approach where the reader delineated volumes of interest only around areas with visually increased tracer activity, and measures of maximal activity recorded. However, this method is sub-optimal [12]. Joshi et al. showed that the difference in the $^{18}$F-sodium fluoride ($^{18}$F-NaF) maximum target-to-background ratio (TBRmax) in culprit compared with non-culprit plaques is only 34% [11]. Additionally, the per plaque TBRmax approach relies on labor-intensive and subjective visual detection of lesions and does not truly reflect disease activity across the entire coronary vasculature. An alternative method for the assessment of $^{18}$F-NaF uptake is the global heart approach which measures activity across the whole heart region [13,14]. The utility of this method, however, is compromised by the inclusion of activity from foci of non-coronary uptake (including the aortic valve and mitral valve annulus) as well as blood pool noise [15].

We here propose a novel semiautomated approach investigating $^{18}$F-NaF uptake throught the entire coronary vasculature using centerlines defined by coronary CT angiography to build 3-dimensional tubular volumes of interest around each of the main epicardial coronary arteries. This method allows evaluation of coronary $^{18}$F-fluoride activity on a per-vessel and per-patient basis, providing more global assessments of disease activity in the coronary arteries. In the initial validation of this new measure, we compare it with the traditional TBRmax approach and assess its relationship with established anatomical quantitative risk indices from CT angiography including low attenuation plaque and coronary artery calcium scoring [2,3].

# Methods

## Patient population

The study was performed on subjects recruited for the ongoing PRE$^{18}$FFIR (Prediction of Recurrent Events with $^{18}$F-Fluoride to Identify Ruptured and High-risk Coronary Artery Plaques in Patients with Myocardial Infarction) trial (NCT02278211). Inclusion required the presence of multi-vessel coronary artery disease on invasive angiography, following recent (within 4 weeks) myocardial infarction. We excluded patients who had a known allergy to iodinated contrast or renal impairment (estimated glomerular filtration rate ≤30 mL/min/1.73 m$^2$) and women of childbearing potential. The study was approved by the local institutional review board, the Scottish Research Ethics Committee (REC reference: 14/SS/0089 and 15/SS/0203), and the United Kingdom (UK) Administration of Radiation Substances Advisory Committee. It was performed in accordance with the Declaration of Helsinki. All patients provided written informed consent prior to any study procedures.

## PET and CT acquisition and reconstruction

All patients underwent $^{18}$F-NaF PET on a hybrid PET-CT scanner (128-slice Biograph mCT, Siemens Medical Systems, Knoxville, USA). All imaging was performed after invasive angiography and revascularization. Prior to imaging, subjects were administered with a target dose of 250 MBq of $^{18}$F-NaF and rested in a quiet environment for 60 minutes. During a single imaging session, we acquired a non-contrast CT attenuation correction scan followed by a 30-min PET emission scan in list mode. The electrocardiography-gated list mode dataset was reconstructed using a standard ordered expectation maximization algorithm with time-of-flight, and point-spread-function correction. Using 10 cardiac gates, we reconstructed the data on a 256×256 matrix (109 slices, slice thickness 2.027mm) using 2 iterations, 21 subsets and 5-mm Gaussian smoothing.

Immediately after the PET scan, a low dose non-contrast (40mAs/rot, 100kV) CT for calculation of the coronary calcium score was performed. Subsequently, a contrast-enhanced coronary CT angiogram was obtained in the same PET/CT system without repositioning the patient. The CT angiography acquisition was conducted according to societal guidelines with the following settings: 330 ms rotation time, 100 or 120kV (depending on body mass index), 160–245 mAs and reconstructed with 0.6 slice thickness and a medium-soft convolution kernel [16].

To compensate for coronary motion associated with heart contraction, we performed cardiac motion correction of the PET/CT images. This technique enables alignment of all gates to the end-diastolic position and as a result allows for inclusion of all PET counts acquired [17].

## Image analysis

**CT—**The Agatston coronary artery calcium score was measured using semiautomatic commercial software (NetraMD, ScImage, Los Altos, CA, USA)[18]. Quantitative plaque analysis of all coronary segments with a lumen diameter ≥2 mm was performed using semi-automated software (AutoPlaque version 2.0, Cedars-Sinai Medical Center, Los Angeles,

USA)[19]. An experienced reader examined coronary CT angiography images in multiplanar format and manually determined the proximal and distal limits of lesions. Subsequent plaque quantification was automated using adaptive scan-specific thresholds. The quantitative presence of LAP was defined as a LAP volume > 0 $mm^3$. The software quantified volumes of the total plaque (TPV), non-calcified plaque (NCP), low-density non-calcified plaque (low attenuation plaque - LAP, attenuation <30 Hounsfield units) and calcified plaque (CP).

**PET—**We used a dedicated software package for coronary PET image analysis (FusionQuant, Cedars Sinai Medical Center, Los Angeles)[20]. PET and CT angiography reconstructions were reoriented, fused and systematically co-registered in all 3 planes [15]. To evaluate $^{18}$F-NaF activity, we used the previously established TBRmax approach (standard quantification) which relies on visual detection of lesions with increased tracer uptake, as well as the newly developed per vessel (and per patient) whole-coronary total microcalcification activity method.

### Standard TBRmax quantification

For a signal to be co-localized to a coronary artery, an atherosclerotic plaque had to be present on the CT angiography and the increased pattern of radiotracer had to arise from the coronary artery and follow its course over >5 mm in three dimensions on orthogonal views [21]. In all plaques which met these criteria, the maximum standardized uptake values (SUVmax) were measured within regions of interest drawn around these areas. To characterize $^{18}$F-NaF coronary uptake in the context of background activity we divided the maximum standard uptake values (SUVmax) by the blood pool activity (mean standard uptake values, SUVmean) measured in the center of the left atrium by delimiting spherical volumes of interest (radius=9–13mm depending on the cavity size) and produced the maximum target to background ratios (TBRmax). We used a 1.25 TBRmax threshold to categorise vessels/plaques as being positive or negative for $^{18}$F-NaF uptake [11].

### Whole coronary $^{18}$F-NaF activity assessment

We devised a novel coronary $^{18}$F-NaF uptake measure based upon the Agatston method for quantifying coronary CT calcium scores and PET quantification techniques widely employed in oncology and cardiac sarcoidosis [22–24]. First, we automatically extracted whole-vessel tubular and tortuous 3D volumes of interest (VOIs) from CT angiography datasets (Figures 1 and S1). These encompass all the main epicardial coronary vessels and their immediate surroundings (4-mm radius) facilitating per-vessel and per-patient uptake quantification. For this study we evaluated $^{18}$F-NaF activity along the entire course of coronary arteries regardless of the presence of coronary stents and we included the left main in the left anterior descending artery VOI. Within such VOIs, we measured the whole vessel SUVmax, and used these to derive TBR values after correction for blood pool. In addition, we explored our novel parameter - the coronary microcalcification activity (CMA)—representing the overall disease activity in the vessel and based upon both the volume and intensity of $^{18}$F-fluoride PET activity within it. CMA was defined as the integrated activity in SUV units exceeding the background blood-pool SUVmean + 2 standard deviations (left atrium activity). The per patient CMA was defined as the sum of the per vessel CMA.

For comparisons between the standard TBRmax and novel whole-coronary quantification approach, we primarily used the maximal standard TBRmax value and CMA at both the per vessel and per patient levels. Analysis of the other quantification measures provided by the whole vessel technique and the standard approach are outlined in the Data Supplement.

**Statistical analysis—**Data were tested for normality using Shapiro Wilks test. Continuous data is expressed as mean (standard deviation) or median [interquartile range] dependent on the distribution. Skewed continuous variables were log transformed to achieve normal distribution. Data were compared with the two-sample t-test. We assessed the associations between two continuous variables using the Pearson's or Spearman's correlation coefficients where appropriate. Correlation coefficients were compared using Fisher's z-transformation. We compared the diagnostic accuracy of uptake measures in detecting LAP with the McNemar test. We used the receiver-operating characteristic analysis and pairwise comparisons according to DeLong et al. to compare the performance of TBRmax and CMA in detecting LAP. A 2-sided p value <0.05 was regarded as significant. Statistical analysis was performed with SPSS software (version 24, SPSS, Inc., Chicago, Illinois).

## Results

### Patients

Fifty patients (64% males, mean age 63±7 years) with recent (range: 8–20 days) myocardial infarction comprised the study cohort (Table 1). All patients had multivessel coronary artery disease and a history of coronary revascularization. Twenty-six subjects (52%) underwent revascularization of more than one vessel.

### Coronary CT angiography

Of the quantitative coronary plaque composition indices, we observed a trend for higher non-calcified plaque (941.7 [632.6, 1552.8] $mm^2$ versus 839.8 [388.9, 1178.1] $mm^2$, p=0.17) and total-plaque volumes (1018.3 [822.6, 1670.3] $mm^2$ versus 897.1 [408.4, 1253.2] $mm^2$, p=0.13) in patients with TBRmax exceeding 1.25. These subjects also showed a trend for higher coronary artery calcium scores (374 [193, 820] versus 213 [88, 466], p=0.07) and had greater LAP volumes (17.9 [3.5, 33.3] $mm^2$ versus 1.4 [0.4, 4.7] $mm^2$, p<0.001) than those with TBRs that did not reach the predefined threshold.

### Positron Emission Tomography

On standard quantification, 41 (82%) subjects had more than one plaque with visually detectable uptake (overall number of plaques with increased activity on visual assessment, range: 0 to 8). Twenty-eight (56%) patients showed uptake exceeding the 1.25 TBRmax threshold. CMA values were higher in patients who met the predefined TBRmax threshold (5.8 [3.5, 10.9] versus 0.2 [0.0, 2.0] p<0.001). There was a strong correlation between CMA and TBRmax values (r=0.76, p<0.001), but CMA had a wider range of values than TBRmax (0 to 12.13 versus 0.80 to 2.44; Figures 2 and 3)

### Associations of CT derived plaque characteristics and $^{18}$F-NaF uptake

Vessels with LAP presented with higher CMA than those without LAP (1.09 [0.02, 2.34] versus 0.0 [0.0, 0.0], p<0.001). While vessel TBRmax was also different in arteries with and without LAP, we observed considerable overlap in uptake values: 1.23 [1.16, 1,37] versus 1.04 [0.93, 1.11], p<0.001 for TBRmax, (Figure 2). Similarly, at the patient level, subjects with LAP presented with higher CMA (3.5 [1.8, 6.5] versus 0.0 [0.0, 0.4], p<0.001) and TBRmax values (1.25 [1.11, 1.46] versus 1.05 [0.95, 1.10], p<0.001 than those without LAP.

In a per-vessel analysis, compared to the 1.25 TBRmax threshold, a CMA greater than 0 had a higher diagnostic accuracy for detection of LAP with a sensitivity of 93.1 (83.3–98.1)% versus 71.6 (56.9–79.4)% and a specificity of 95.7 (88.0–99.1)% versus 80.0 (68.7–88.6)% (both p<0.001; Tables 2 and 3, Figure 4). Compared to TBRmax and coronary artery calcium score, CMA also had a higher area under the ROC curve for detection of LAP (0.95, 95% CI: 0.90 to 0.99 versus 0.85, 95% CI: 0.80 to 0.90 and 0.67, 95% CI: 0.60 to 0.74 respectively; p<0.001).

Of the quantitative plaque characteristics, only LAP volume and coronary artery calcium score correlated with $^{18}$F-NaF uptake. In particular, we observed a strong correlation between LAP volume and CMA at both the per vessel (r=0.84, p<0.001) and per patient (r=0.86, p<0.001) levels (Figure 5). In contrast, the associations between LAP volume and TBRmax were only moderate (per-vessel r=0.56, p<0.001; per-patient r=0.63, p<0.001 respectively). Coronary artery calcium score was only moderately associated with TBRmax and CMA both on the per vessel (r=0.30, p=0.001 versus r=0.39, p<0.001) and per patient level (r=0.38, p=0.01 versus r=0.43, p=0.003). Associations between LAP volume and, SUVmax, averaged-SUVmax, and averaged-TBRmax were all weaker than with CMA and TBRmax both at the per vessel and per patient levels (data supplement results and Figures S2–4).

## Discussion

In this study, we describe a novel, dedicated approach for measuring disease activity across the coronary vasculature. By leveraging CT angiography-derived whole-vessel 3-dimensional volumes of interest, we were able to express $^{18}$F-NaF PET tracer activity as the global CMA mimicking an approach successfully implemented in the field of oncology and cardiac sarcoidosis [22–24]. Indeed, CMA represents both the volume and intensity of coronary $^{18}$F-NaF activity, similar to the Agatston method for CT calcium scoring. Rather than being limited to reporting the highest SUV, TBR or the number of plaques with increased tracer activity, CMA reflects the whole-coronary $^{18}$F-NaF uptake burden which can be compared with total coronary burden of various plaque components on CT angiography. As a result, in patients and vessels with multiple foci of uptake, CMA provides a continuous measure of disease activity across the coronary vasculature. The proposed approach moves away from a single hot spot approach to a patient level total $^{18}$F-NaF activity burden assessment and hence does not rely on a single-pixel-value as traditional uptake measures (TBR or SUV). Moreover, our whole vessel method omits the need for time consuming and subjective manual delineation of lesions and only requires careful co-registration of the PET and CT angiography datasets [15].

We have previously shown that TBRmax of $^{18}$F-NaF is associated with LAP [25]. Here we show that CMA outperformed the hot-spot TBRmax approach for the detection of LAP. Similarly, we found a stronger correlation between LAP and CMA than LAP and conventional measurements of $^{18}$F-NaF activity, and better categorical separation. Given that LAP has repeatedly been shown to be associated with adverse outcome, the discrepancy in the correlations and diagnostic accuracy of LAP and CMA versus TBR/SUV supports the view that in characterizing disease severity, CMA is superior than traditional uptake measures [19].

The assessment of the whole-coronary disease burden is of great importance as over the past decade the ongoing pursuit of the vulnerable plaque has proved to be elusive [2]. To date, several studies have already shown that adverse plaque features (LAP, positive remodeling) observed on CT angiography are predictors of adverse events [6–8]. Despite initial enthusiasm, the low predictive value of individual plaques progressing to cause events has emerged as the major limitation of the vulnerable plaque strategy [4,5]. In view of these limitations, advanced invasive and non-invasive imaging is moving towards distinguishing vulnerable patients rather than detecting individual vulnerable plaques [2,3].

Since coronary $^{18}$F-NaF imaging is being potentially considered as a non-invasive tool for imaging high-risk coronary artery disease, we aimed to develop a quantification approach that would be in line with the vulnerable patient rather than the vulnerable plaque paradigm. Current coronary PET reporting does not provide insights into global coronary $^{18}$F-NaF burden. By reporting only the highest TBRmax values, overall coronary activity cannot be appreciated. Indeed, this approach can be misleading as it can underestimate the $^{18}$F-NaF burden in individuals with multiple foci of uptake in their coronary vasculature (Figure 3). In addition, by identifying the coronary artery boundaries from CT angiography and confining the assessment of $^{18}$F-NaF within these boundaries, the CMA approach has the potential to reduce the subjectivity and the time required for image analysis.

The global cardiac method is an alternative, previously proposed approach for cardiac $^{18}$F-NaF analysis [12]. This technique requires VOIs to be drawn around the cardiac silhouette on consecutive axial slices of fused PET/CT images and maximum radiotracer activity is recorded for each slice. However, the global cardiac uptake method relies on the assumption that any cardiac $^{18}$F-NaF activity detected as higher than blood pool originates from the coronary vasculature. There is accumulating evidence that cardiac valves and great vessels bind $^{18}$F-NaF [20,26]. Additionally, increased myocardial uptake of $^{18}$F-NaF is often observed in the infarcted myocardium, myocardial scar tissue and cardiac amyloidosis [27–29]. All of these may falsely elevate the global $^{18}$F-NaF reading leading to overestimation of coronary $^{18}$F-NaF activity. Compared to the global cardiac method, the approach we propose herein is highly specific (as only uptake originating from coronary arteries is being quantified) and therefore provides a global measure of coronary disease activity without contamination from surrounding structures.

In oncology and in the field of cardiac sarcoidosis, similar concerns surround SUVmax reporting. It was argued that SUV measurements are prone to several patient and scan protocol factors and are only accurate when there is homogeneous uptake in the tumor [25].

As a result, new quantitative approaches have been proposed. Rather than evaluating individual lesions, these approaches shifted towards metrics that better represent the patient's total tumor load, such as the total metabolic active tumor volume [30–32]. Importantly these new measures have been found to predict disease progression, recurrence, and death [33,34]. Ahmadian and colleagues developed a quantitative measure of $^{18}$F-fluorodeoxyglucose volume intensity called Cardiac Metabolic Activity [24]. In patients with suspected cardiac sarcoidosis, this approach was independently associated with future events. In our study, we employed a method based on this oncological approach for quantification of coronary PET. We showed that compared to the local TBR or SUV based approach, it offers better in-depth characterization of the $^{18}$F-NaF burden and is more closely associated with established CT angiography derived markers of unfavorable prognosis (LAP) than the conventional approach.

### Limitations

Our study lacks outcome data and thus we were unable to validate the whole-vessel uptake measurements with clinical endpoints. Instead, we employed established high-risk quantitative plaque features evaluated on CT angiography as a surrogate. Although mechanistically attractive, correlating $^{18}$F-NaF uptake measurements with quantitative coronary lesion analysis indices is suboptimal in patients who underwent coronary revascularization. While quantification of $^{18}$F-NaF uptake is not hampered by the presence of coronary stents, the assessment of plaque composition is not feasible in stented segments of arteries. Because the study cohort was comprised of subjects with recent myocardial infarction, all subjects had a medical history of coronary interventions (Figure S5). While we have shown that delayed $^{18}$F-NaF imaging facilitates image analysis, participants in this study underwent PET imaging 1 h after tracer injection and thus our whole vessel image uptake analysis remains to be tested with delayed imaging in the future [35].

## Conclusions

Automated whole-vessel $^{18}$F-NaF coronary microcalcification activity assessment with CT angiography-guided 3-dimensional volumes of interest is feasible and provides a direct measure of the disease activity in each vessel and total disease burden for the patient. This approach correlates better than traditional measures of uptake with low attenuation plaque - an established anatomical marker of vulnerability.

## Supplementary Material

Refer to Web version on PubMed Central for supplementary material.

## Funding:

This research was supported in part by grants R01HL135557 and R01HL133616 from the National Heart, Lung, and Blood Institute/National Institute of Health (NHLBI/NIH) and by a grant from the Dr. Miriam & Sheldon G. Adelson Medical Research Foundation. The content is solely the responsibility of the authors and does not necessarily represent the official views of the National Institutes of Health.

## Abbreviations and acronyms

| | |
|---|---|
| **CAD** | Coronary Artery Disease |
| **CMA** | Coronary Microcalcification Activity |
| **CI** | Confidence Intervals |
| **CT** | Computed Tomography |
| **PET** | Positron Emission Tomography |
| **SD** | Standard Deviation |
| **SUVmax** | Maximum Standard Uptake Value |
| **TBRmax** | Maximum Target to Background Ratio |
| **$^{18}$F-NaF** | $^{18}$F-sodium Fluoride |

## References:


1. Go AS, Mozaffarian D, Roger VL, et al. for the American Heart Association Statistics Committee and Stroke Statistics Subcommittee (2014) Heart disease and stroke statistics—2014 update: a report from the American Heart Association. Circulation 129:e28–e292 [PubMed: 24352519]
2. Arbab-Zadeh A, Fuster V. The Myth of the “Vulnerable Plaque” J Am Coll Cardiol 2015, 65 (8) 846–855; DOI: 10.1016/j.jacc.2014.11.041 [PubMed: 25601032]
3. Dweck MR, Aikawa E, Newby DE, Tarkin JM, Rudd JH, Narula J, Fayad ZA. Noninvasive molecular imaging of disease activity in atherosclerosis. Circ Res. 2016; 119:330–340. doi: 10.1161/CIRCRESAHA.116.307971. [PubMed: 27390335]
4. Stone GW, Maehara A, Lansky AJ,et al. A prospective natural-history study of coronary atherosclerosis. N Engl J Med. 2011; 364:226–235. doi: 10.1056/NEJMoa1002358 [PubMed: 21247313]
5. Calvert PA, Obaid DR, O’Sullivan M et al. Association between IVUS findings and adverse outcomes in patients with coronary artery disease: the VIVA (VH-IVUS in Vulnerable Atherosclerosis) Study. JACC Cardiovasc Imaging. 2011; 4:894–901. doi: 10.1016/j.jcmg.2011.05.005 [PubMed: 21835382]
6. Williams MC, Moss AJ, Dweck M et al. Coronary artery plaque characteristics associated with adverse outcomes in the SCOT-HEART study. J Am Coll Cardiol 2019;73:291–301. [PubMed: 30678759]
7. Ferencik M, Mayrhofer T, Bittner DO, et al. Use of high-risk coronary atherosclerotic plaque detection for risk stratification of patients with stable chest pain: a secondary analysis of the PROMISE randomized clinical trial. JAMA Cardiol 2018;3:144–152. [PubMed: 29322167]
8. Nerlekar N, Ha FJ, Cheshire C, Rashid H et al. Computed tomographic coronary angiography–derived plaque characteristics predict major adverse cardiovascular events: a systematic review and meta-analysis.Circ Cardiovasc Imaging. 2018; 10:e006973. doi: 10.1161/CIRCIMAGING.117.006973
9. Rudd JHF, Warburton EA, Fryer TD et al. Imaging atherosclerotic plaque inflammation with F-18 -fluorodeoxyglucose positron emission tomography. Circulation, 105(23), 2708–2711. doi:10.1161/01.cir.0000020548.60110.76
10. Tarkin JM, Joshi FR, Evans NR et al. Detection of Atherosclerotic Inflammation by (68)Ga-DOTATATE PET Compared to [(18)F]FDG PET Imaging. J Am Coll Cardiol, 69(14), 1774–1791. doi:10.1016/j.jacc.2017.01.060

11. Joshi NV, Vesey AT, Williams MC et al. F-18-fluoride positron emission tomography for identification of ruptured and high-risk coronary atherosclerotic plaques: a prospective clinical trial. Lancet, 383(9918), 705–713. doi:10.1016/s0140-6736(13)61754-7
12. Bellinge JW, Francis RJ, Majeed K et al. In search of the vulnerable patient or the vulnerable plaque: (18)F-sodium fluoride positron emission tomography for cardiovascular risk stratification. J Nucl Cardiol 2018 10.1007/s12350-018-1360-2.
13. Beheshti M, Saboury B, Mehta N. Detection and global quantification of cardiovascular molecular calcification by fluoro-18-fluoride positron emission tomography/computed tomography—A novel concept. Hell J Nucl Med 2011;14:114–20. [PubMed: 21761011]
14. Blomberg BA, Thomassen A, de Jong PA et al. Impact of personal characteristics and technical factors on quantification of sodium 18F-fluoride uptake in human arteries: Prospective evaluation of healthy subjects. J Nucl Med 2015;56:1534–40. [PubMed: 26205304]
15. Kwiecinski J, Adamson PD, Lassen ML et al. Feasibility of coronary 18F-sodium fluoride PET assessment with the utilization of previously acquired CT angiography. 2018 Circ Cardiovasc Imaging 11(12): e008325 [PubMed: 30558496]
16. Leipsic J, Abbara S, Achenbach S, Cury R, Earls JP, Mancini GJ et al. SCCT guidelines for the interpretation and reporting of coronary CT angiography: a report of the Society of Cardiovascular Computed Tomography Guidelines Committee. JCCT 2014;8:342–58
17. Rubeaux M, Joshi N, Dweck MR et al. Motion correction of 18F-sodium fluoride PET for imaging coronary atherosclerotic plaques. J Nucl Med. Society of Nuclear Medicine; 2015 10 15;:jnumed.115.162990.p
18. Agatston AS, Janowitz WR, Hildner FJ, Zusmer NR, Viamonte M Jr, Detrano R. Quantification of coronary artery calcium using ultrafast computed tomography. J Am Coll Cardiol 1990;15:827–32. [PubMed: 2407762]
19. Hell MM, Motwani M, Otaki Y et al. Quantitative global plaque characteristics from coronary computed tomography angiography for the prediction of future cardiac mortality during long-term follow-up. Eur Heart J Cardiovasc Imaging 2017;18:1331–1339. [PubMed: 28950315]
20. Massera D, Doris MK, Cadet S et al. Analytical quantification of aortic valve 18F-sodium fluoride PET uptake. J Nucl Cardiol. 2018 11 29. doi: 10.1007/s12350-018-01542-6. [Epub ahead of print]
21. Doris MK, Otaki Y, Krishnan SK, Kwiecinski J, Rubeaux M, Alessio A et al. Optimization of reconstruction and quantification of motion-corrected coronary PET-CT. J Nucl Cardiol 2018; epub ahead of print
22. Rahim MK, Kim SE, So H et al. Recent Trends in PET Image Interpretations Using Volumetric and Texture-based Quantification Methods in Nuclear Oncology. Nuclear medicine and molecular imaging, 48(1), 1–15. doi:10.1007/s13139-013-0260-2
23. Steven ML, Yusuf E, Timothy A et al. Tumor Treatment Response Based on Visual and Quantitative Changes in Global Tumor Glycolysis Using PET-FDG Imaging: The Visual Response Score and the Change in Total Lesion Glycolysis. Clinical Positron Imaging, 2 (3): 159–171
24. Ahmadian A, Brogan A, Berman J, et al. Quantitative interpretation of FDG PET/CT with myocardial perfusion imaging increases diagnostic information in the evaluation of cardiac sarcoidosis. J Nucl Cardiol 2014;21:925–39. doi:10.1007/s12350-014-9901-9 [PubMed: 24879453]
25. Kwiecinski J, Dey D, Cadet S et al. Predictors of 18F-sodium fluoride uptake in patients with stable coronary artery disease and adverse plaque features on computed tomography angiography. Eur Heart J Cardiovasc Imaging. 2019 6 18 pii: jez152. doi: 10.1093/ehjci/jez152. [Epub ahead of print]
26. Forsythe RO, Dweck MR, McBride OMB, et al. F-18-Sodium Fluoride Uptake in Abdominal Aortic Aneurysms The SoFIA(3) Study. J Am Coll Cardiol, 71(5), 513–523. doi:10.1016/j.jacc.2017.11.053.
27. Han JH, Lim SY, Lee MS, et al. Sodium [18F]fluoride PET/CT in myocardial infarction. Mol Imaging Biol 2015;17:214–21. [PubMed: 25281410]
28. Giovanna Trivieri M, Dweck MR, Abgral R, Robson PM et al. 18F-sodium fluoride PET/MR for the assessment of cardiac amyloidosis. J Am Coll Cardiol 2016;68:2712–4. [PubMed: 27978955]

29. Marchesseau S, Seneviratna A, Sjöholm AT et al. Hybrid PET/CT and PET/MRI imaging of vulnerable coronary plaque and myocardial scar tissue in acute myocardial infarction. J Nucl Cardiol 2017.

30. Chen HHW, Chiu N-T, Su W-C et al. Prognostic value of whole-body total lesion glycolysis at pretreatment FDG PET/CT in non–small cell lung cancer. Radiology. 2012;264(2):559–66. [PubMed: 22692034]

31. Frings V, van Velden FHP, Velasquez LM et al. Repeatability of metabolically active tumor volume measurements with FDG PET / CT in advanced gastrointestinal malignancies: a multicenter study. Radiology. 2014;273(2):539–48. [PubMed: 24865311]

32. Kramer GM, Frings V, Hoetjes N et al. Repeatability of quantitative whole-body 18F-FDG PET/CT uptake measures as function of uptake interval and lesion selection in non-small cell lung cancer patients. J Nucl Med. 2016;57(9):1343–9. [PubMed: 27103020]

33. Lee P, Weerasuriya DK, Lavori PW et al. Metabolic tumor burden predicts for disease progression and death in lung cancer. Int J Radiat Oncol Biol Phys. 2007;69(2):328–33. [PubMed: 17869659]

34. La TH, Filion EJ, Turnbull BB et al. Metabolic tumor volume predicts for recurrence and death in head-and-neck cancer. Int J Radiat Oncol Biol Phys. 2009;74(5):1335–41. [PubMed: 19289263]

35. Kwiecinski J, Berman DS, Lee SE et al. Three-hour delayed imaging improves assessment of coronary 18F-sodium fluoride PET. Journal Nuclear Medicine jnumed.118.217885 published ahead of print 9 13, 2018

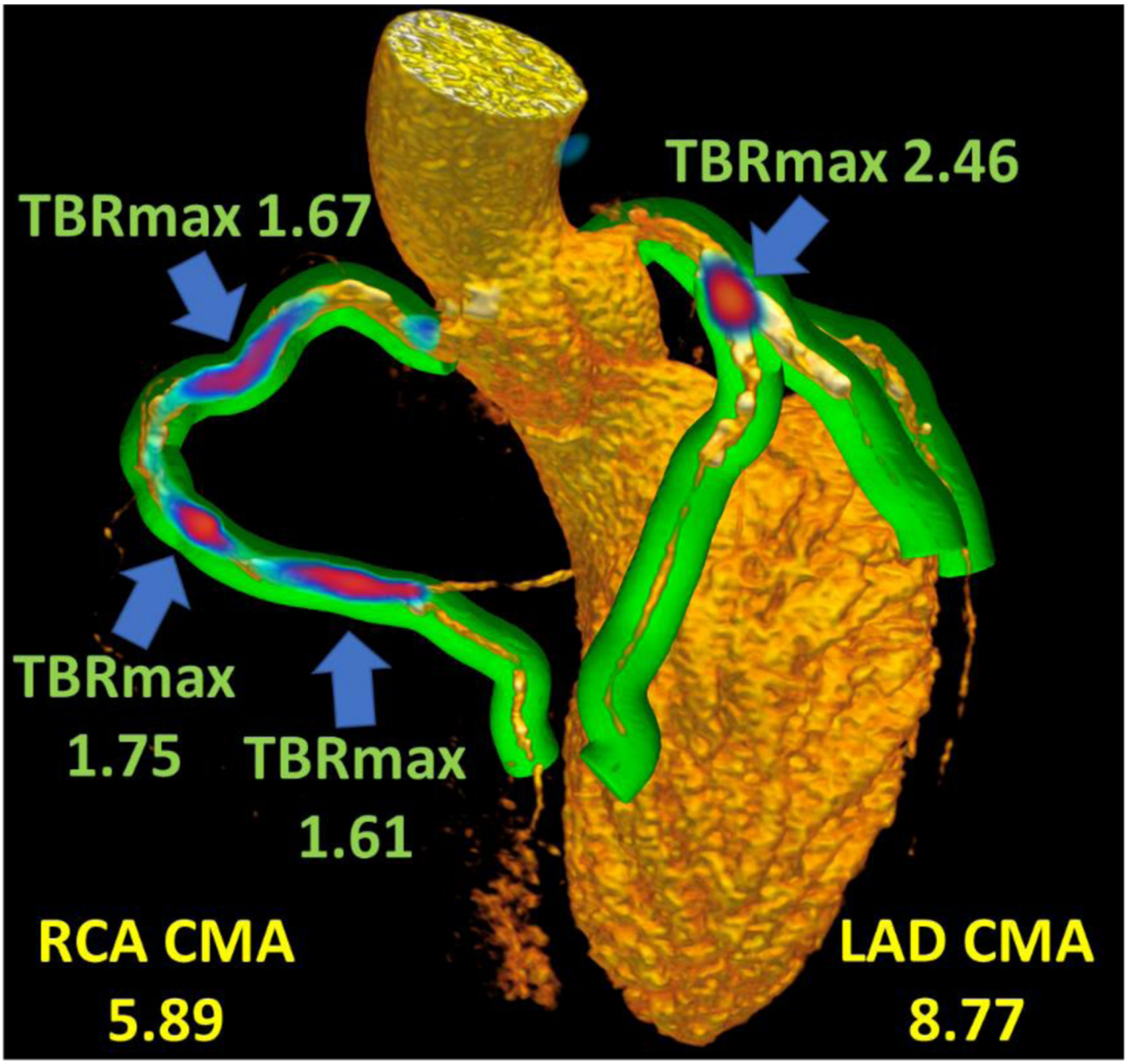


**Figure 1.**

3-dimensional rendering of coronary CT angiography with superimposed tubular whole vessel volumes of interest (light green) employed for evaluation of $^{18}$F-sodium fluoride uptake (blue and red). Despite the relatively lower tissue-to-background ratio maximum (TBRmax) due to multiple foci of increased $^{18}$F-NaF activity, the coronary microcalcification activity (CMA) in the right coronary artery (RCA) is only moderately lower than in the left anterior descending (LAD) coronary artery which presented with a very high TBRmax.

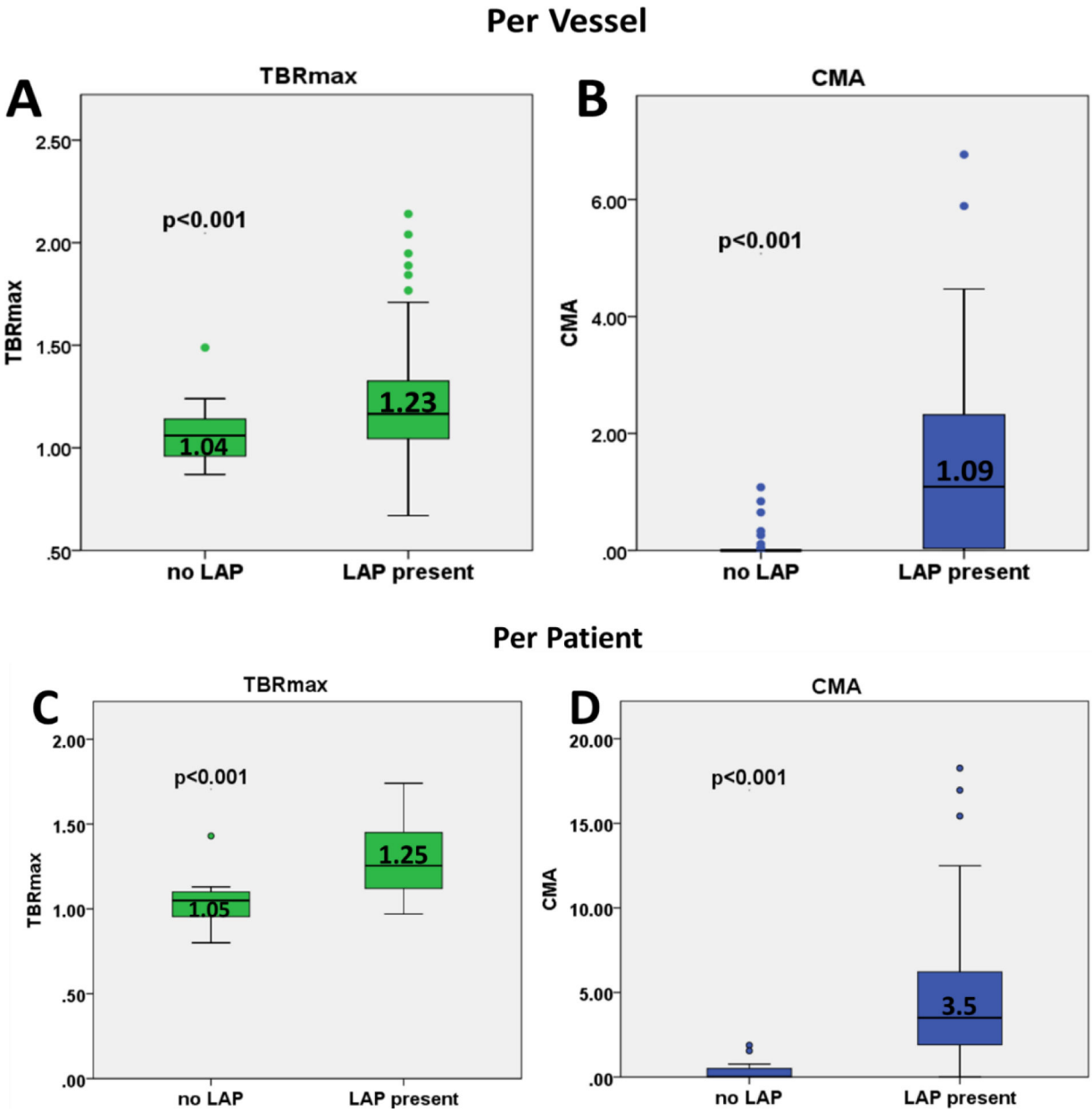


**Figure 2.**

Coronary microcalcification activity (CMA) versus maximum target-to-background ratio (TBRmax) values of $^{18}$F-sodium fluoride uptake. Per vessel (n=142) TBRmax (A) and CMA (B) values in arteries with and without low attenuation plaque (LAP) on quantitative plaque analysis. Per patient (n=50) TBRmax (C) and CMA (D) values in patients with and without LAP on quantitative coronary plaque analysis.

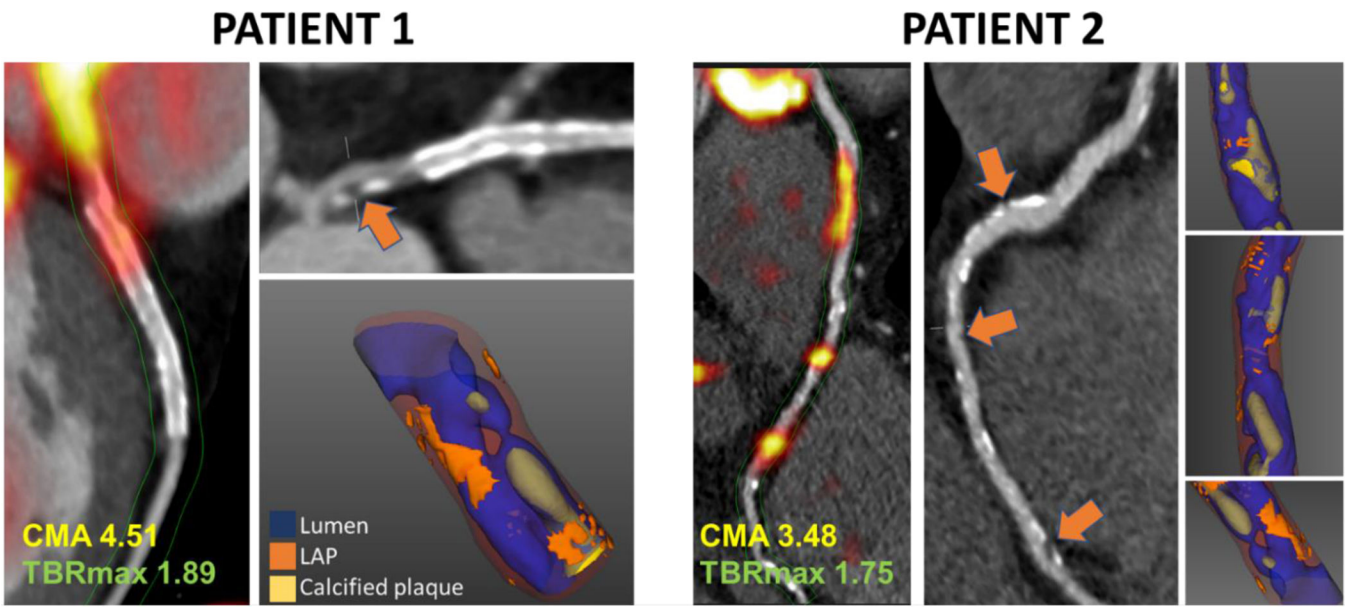


**Figure 3.**

Case examples of coronary $^{18}$F-sodium fluoride uptake, low attenuation plaque (LAP) on CT angiography and LAP (orange arrows, II) on 3D CT rendering (III). Right (Patient 1) and left anterior descending (Patient 2) coronary arteries. Areas of LAP correspond with areas of increased $^{18}$F-NaF activity. While maximum target-to-background ratio (TBRmax) reflects single hot-spot activity coronary microcalcification activity (CMA) values represent the whole-vessel $^{18}$F-sodium fluoride burden.

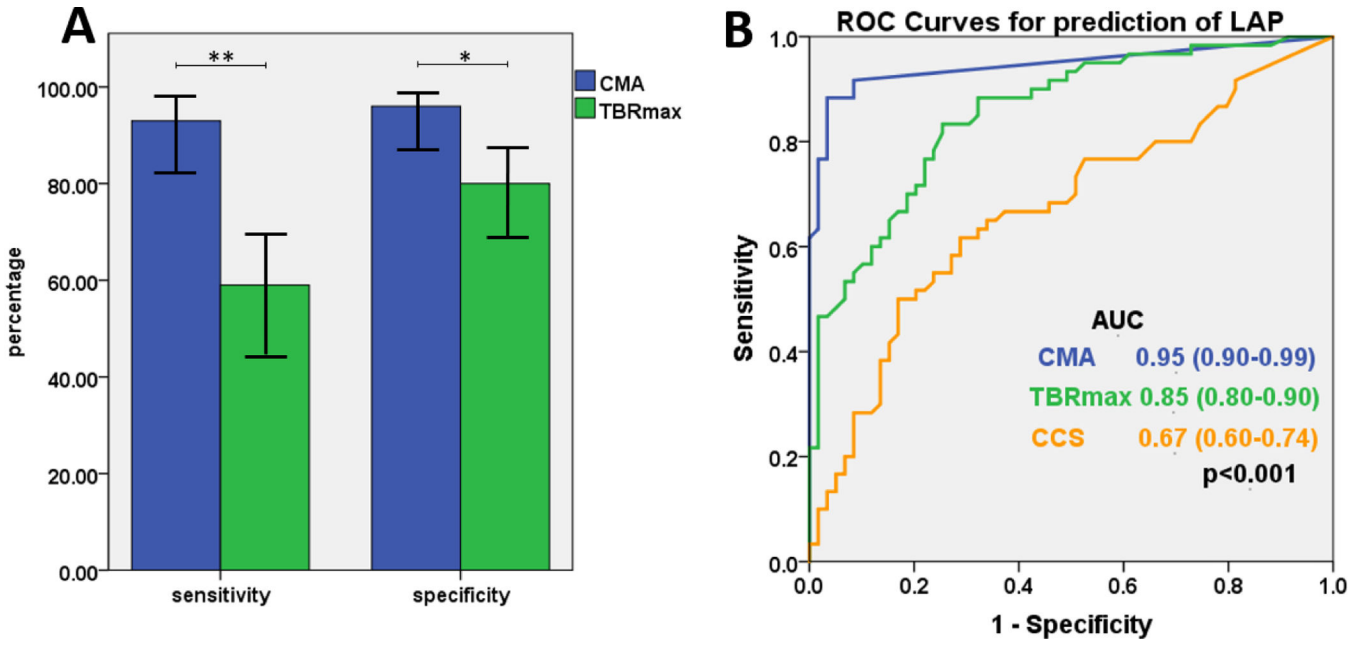


**Figure 4.**

The diagnostic performance of coronary microcalcification activity (CMA) and maximum target-to-background (TBRmax) in detecting low attenuation plaque (LAP). (A) The sensitivity, specificity of the 1.25 TBRmax threshold and CMA greater than 0 for predicting LAP on quantitative plaque analysis. CMA had a higher sensitivity, specificity than the TBRmax threshold (all p<0.001). (B) Receiver operator curves for detection of LAP using CMA, TBRmax and coronary artery calcium scores. CMA had a higher area under the curve (AUC) than TBRmax and CCS (p<0.001).

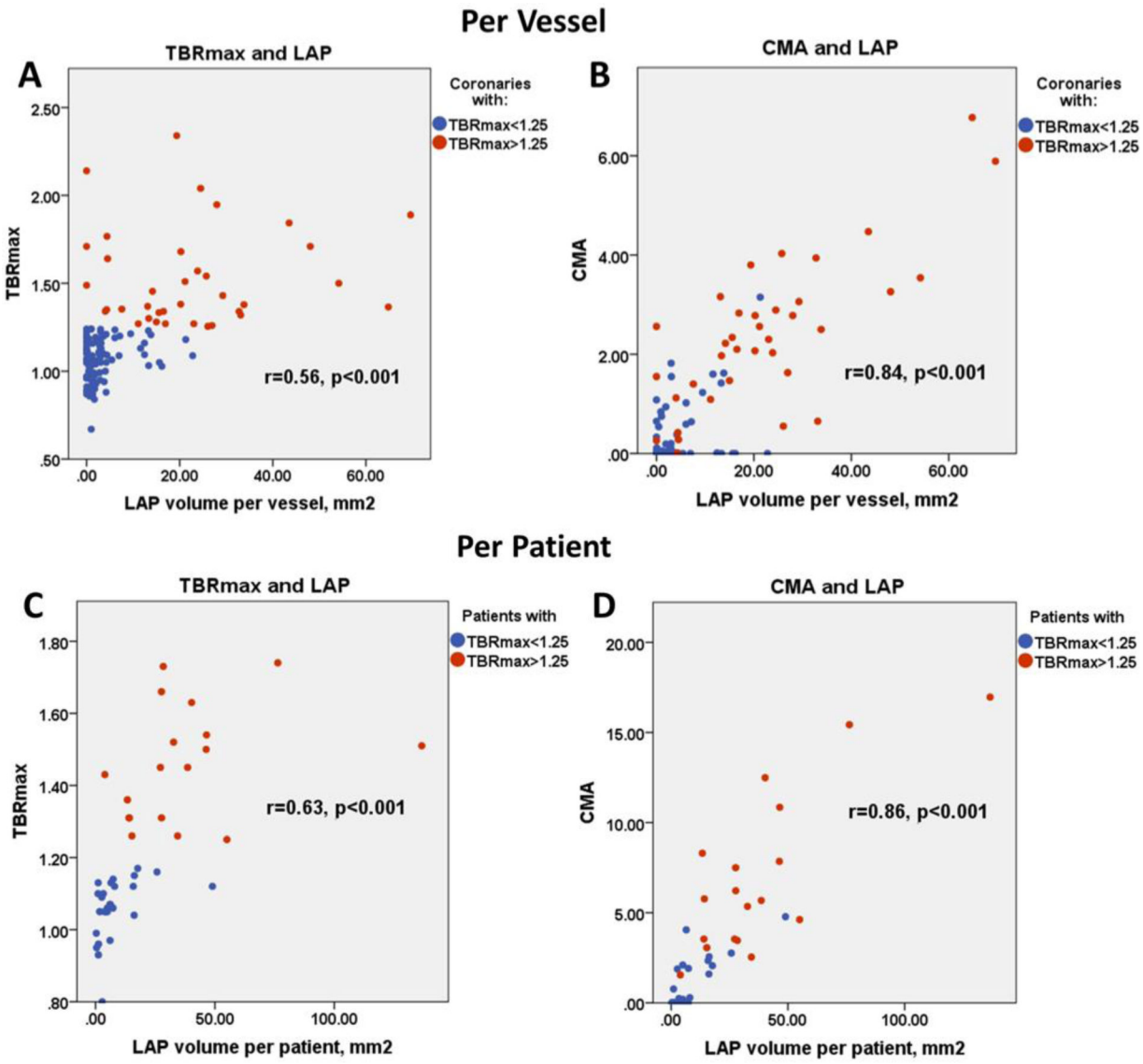


**Figure 5.**

Coronary $^{18}$F-sodium fluoride uptake and low attenuation plaque volume (LAP) on quantitative coronary plaque analysis. Per vessel: (A) maximum target-to-background (TBRmax) and LAP volume. (B) Coronary microcalcification activity (CMA) and LAP volume. Per patient: (C) TBRmax and LAP volume. (D) CMA and LAP volume.

**Table 1.**

Baseline Characteristics of Study Patients.

| **Baseline Characteristics** | |
|---|---|
| Age, years | 63±7 |
| Males, n (%) | 32 (64%) |
| Diabetes, n (%) | 4 (8%) |
| Hyperlipidemia, n (%) | 40 (80%) |
| Hypertension, n (%) | 39 (78%) |
| Tobacco use, n (%) | 4 (8%) |
| Family history of CAD, n (%) | 12 (24%) |
| **Medications** | |
| Aspirin, n (%) | 19 (38%) |
| Clopidogrel, n (%) | 10 (20%) |
| Statin, n (%) | 23 (46%) |
| ACEI/ARB, n (%) | 17 (34%) |
| Beta Blocker, n (%) | 8 (16%) |
| **Coronary Computed Tomography Angiography** | |
| Segment involvement score | 6 [5, 8] |
| Multivessel disease, n (%) | 50 (100%) |
| Coronary artery calcium score | 113 [90, 387] |
| Total plaque volume ($mm^3$) | 963 [670, 1120] |
| NCP volume ($mm^3$) | 858 [574, 1041] |
| Low attenuation plaque ($mm^3$) | 9 [0.0, 14] |
| **PET/CT** | |
| SUVmax | 1.5 [1.2, 1.6] |
| TBRmax | 1.3 [1.1, 1.4] |
| CMA | 1.2 [0.3, 1.7] |
| Background SUVmean | 1.1 [1.0, 1.2] |

CAD – coronary artery disease, CMA – coronary microcalcification activity, HDL – high-density lipoprotein, LDL – low-density lipoprotein, NCP – non-calcified plaque, SUVmaxSUVmean – maximum/mean standard uptake value, TBRmax – maximum target to background ratio

**Table 2.**

The discriminatory performance of $^{18}$F-NaF uptake thresholds for distinguishing vessels with LAP on quantitative plaque analysis. TBRmax 1.25 threshold (A). CMA greater than 0 (B). (B).

| **A** | | | |
|---|---|---|---|
| | **TBRmax>1.25** | **TBRmax<1.25** | |
| LAP>0 | 34 | 24 | 58 |
| LAP=0 | 14 | 56 | 70 |
| | 48 | 80 | |
| **B** | | | |
| | **CMA>0** | **CMA=0** | |
| LAP>0 | 54 | 4 | 58 |
| LAP=0 | 3 | 67 | 70 |
| | 57 | 71 | |

**Table 3.**

The sensitivity, specificity, positive and negative predictive value of the 1.25 maximum target to background (TBRmax) threshold and coronary microcalcification activity (CMA) greater than 0 for predicting low attenuation plaque (LAP) on quantitative plaque analysis. CMA had a significantly higher sensitivity, specificity, positive and negative predict value than the TBRmax threshold (all $p<0.001$).

| 18F-NaF uptake measure | Sensitivity (95% CI) | Specificity (95% CI) | Positive predictive value (95% CI) | Negative predictive value (95% CI) |
|---|---|---|---|---|
| TBRmax | 71.6 (56.9–79.4) | 80.0 (68.7–88.6) | 70.8 (59.2–80.3) | 69.7 (62.7–76.4) |
| CMA | 93.1 (83.3–98.1) | 95.7 (88.0–99.1) | 94.7 (85.6–98.2) | 94.4 (86.7–97.7) |

CI – confidence interval;